



## DYNAMIC OF ACTIVE MAGNETIC BEARINGS

**Luiz de Paula do Nascimento**

Departamento de Engenharia Mecânica  
Faculdade de Engenharia de Ilha Solteira  
Av. Brasil, 56 – 15385-000 – Ilha Solteira – SP  
E-mail: [depaula@dem.feis.unesp.br](mailto:depaula@dem.feis.unesp.br)

***Abstract:** The oscillatory motion of any rotor-bearing system is defined by the amount of stiffness and damping present. With mechanical bearing, stiffness and damping characteristics are generally fixed by the design of the bearing. In contrast, the stiffness and damping characteristics of the magnetic bearings are adjusted through the choice of control system parameters for a given control algorithm. This provides the ability to significantly change the system dynamics within the bounds of physical and operating constraints. Thus, in this article the author presents a general discussion of the operation of an active magnetic bearing, as well as the procedure to calculate the stiffness and damping from a set of control system parameters for rotor dynamic purposes.*

***Keywords:** Active Magnetic Bearing, Modeling, Rotor Dynamic System*

### 1. INTRODUCTION

Active Magnetic Bearing (AMB) is a rather new concept in bearing technology. The AMBs are electromagnetic devices configured to suspend a shaft within a gap. The basic operating principles of AMBs are given in Allaire et al (1993). They take radial loads or thrust loads by utilizing a magnetic field to support the shaft rather than a mechanical force as in fluid film or rolling element bearings.

Magnetic bearings provide several advantages over conventional bearings for a variety of practical applications. One of these advantages is no lubrication requirement that results in the reduction of equipment maintenance, waste associated with the replacement of used lubricants and bearings. Besides, the AMBs are well suited to applications such as canned pumps, turbomolecular vacuum pumps, turboexpanders, and centrifuges where oil cannot be employed. Because there is no contact between the rotor and stator, there is no wear and bearings commonly have lower power consumption and very long life. Another advantage of AMBs is that they are capable of operating under much higher speeds than conventional rolling element bearings with relatively low power losses. Also, they can operate at much higher temperatures or at much lower temperatures than oil lubricated bearings. One great benefit of the AMBs is that they also have active vibration control capabilities. Schweitzer and Lange (1976) recognized the potential for active vibration control of rotor using AMB technology. Since then, significant work in the active vibration control area has been completed.

One potential disadvantage is that AMBs have a lower load capability than conventional bearings, and therefore, need a larger envelope for installation. Economics plays a large role in

dictating and limiting the use of AMBs. A long-term payback analysis including reduction of maintenance costs is necessary for economic justification in some cases.

An overview of active magnetic bearing applications has been presented in Kasarda (2000). In commercial applications, pumps and turbomachinery with nominal operating speeds as high as 60,000 rpm have represented the majority of equipment outfitted with AMBs. Also, there are many promising new AMB research topics under investigation. Examples of some of these research topics are bearingless motors, biomedical applications (external blood pumps and artificial heart designs), machine tool research, aircraft jet engines, flywheel energy storage systems and miniaturized systems. The application in big installations also is under investigation. Yamaishi (1997) presents the application of magnetic bearing for water turbine and generator. There are several works on application of AMBs as actuator in active and adaptive vibration control system (Hope, 1997; Knospe, 1993; Beale, 1992; Redmond, 1992; Nonami, 1998; Ku, 1993).

In rotating machinery applications, always it is very important to know how the AMBs affect the rotor dynamic to determine a set of control parameters that induces a safe dynamic stability.

## 2. ACTIVE MAGNETIC BEARING THEORY

In the theoretical model of the magnetic bearings several assumptions are made in the following: 1) flux levels are always below saturation level; 2) shaft motions are small compared to the steady state air gap dimension; 3) the flux distribution is relatively uniform in stator cross sections, and; 4) leakage is small. Some of these assumptions may be violated by a particular bearing design, but this does not mean that the bearing will not operate. In general, a reliable finite element analysis must be carried out.

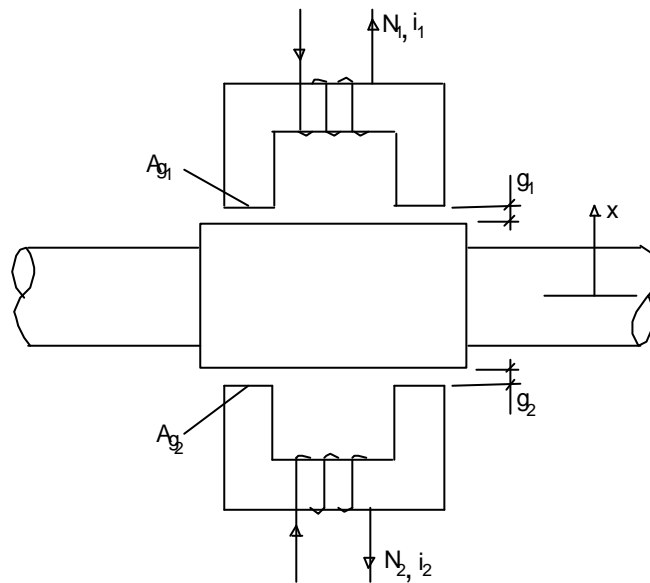


Figure 1. Basic geometry of a double acting magnetic actuator

The magnetic part of the circuit, as illustrated in the Fig. (1), is constructed of magnetic material such as silicon steel or higher saturation level magnetic materials such as Vanadium Permendur. Magnetic flux is produced in each horseshoe shaped section of the bearing. Magnetic bearings are normally constructed of a ferrous magnetic material and the air gaps made as small as practical to minimize the required magnetomotive force. Nearly always, the magnetic flux in magnetic bearings is determined by the air gap and the reluctance of the magnet iron can be neglected compared to that in the air gap. The typical ferrous magnetic material employed in a magnetic actuator has a magnetization curve, plotted as magnetic flux density ( $B$ ) vs. magnetic field intensity ( $H$ ), as illustrated in Fig. (2). The  $B-H$  curve is roughly linear for much of the range of  $B$ . The slope of this

curve in the linear range is called the permeability of the material,  $\mu$ . Often, this is expressed as the product of the permeability of the free space (air gap),  $\mu_0$ , times a relative permeability for the material,  $\mu_r$ . The  $B$ - $H$  relation is,

$$B = \mu_0 \mu_r H \quad (1)$$

At higher values of  $B$ , the  $B$ - $H$  curve is no longer linear. The knee of the curve is called the saturation point. For silicon steel, this typically occurs in the range of 1.5 to 1.7 Tesla (1 Tesla = 10,000 Gauss). With the advanced magnetic materials such as Vanadium Permendur, this value may be as high as 2.2 to 2.4 Tesla. When the bearing operation drives the material to that point, it acts as if it has an air core. The required magnetomotive force is then quite high and not economical.

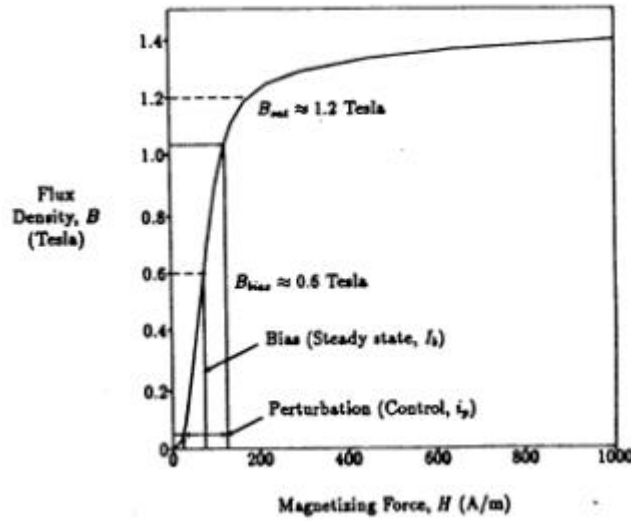


Figure 2. Magnetic flux density ( $B$ ) vs. magnetic field intensity ( $H$ ) for silicon iron

The force  $F_g$  per air gap of thickness  $g$  and area  $A_g$ , which attract the rotor to the stator and permit the actuator to act as a bearing, is given by,

$$F_g = e \frac{B^2 A_g}{2\mu_0} = e \frac{\mu_0 N^2 i^2 A_g}{8g^2} \quad (2)$$

where  $e$  is a geometric correction factor of the fringing and leakage effects and  $N$  is the number of wires wrapped around a closed magnetic path carrying current  $i$ . There are actually two air gaps in the bearing circuit, so the total force is twice this value, then,

$$F = e \frac{B^2 A_g}{\mu_0} = e \frac{\mu_0 N^2 i^2 A_g}{4g^2} \quad (3)$$

The force is proportional to the square of  $Ni$  and inversely proportional to the square of gap  $g$ . It would appear from this result that magnetic bearings are very nonlinear devices. However, a close examination of a double acting bearing reveals a different result.

Actual operation of the magnetic bearing involves superposition of two fluxes: a bias flux and a perturbation flux, as shown in Fig. (2). The bias flux density  $B_b$  is a steady state flux level induced in the air gap by a bias  $i_b$  (steady state) current in the coil. The perturbation flux density  $B_p$  is a time

varying control flux density developed by the perturbation (control) current  $i_p$  in the coil. The total fluxes and currents in the coils are,

$$B = B_p + B_b \quad \text{and} \quad i = i_b + i_p \quad (4)$$

Usually, the bias flux level  $B_b$  is set at about one half of the magnetic saturation level, shown in Fig. (2), allowing for relatively large perturbation flux levels up and down from the bias level.

Electromagnetic forces are only attractive, so actuators must be placed on both sides of the moving components in a double acting arrangement, as illustrated in Fig. (1). From Eq. (3), the net force  $F_N$  is given by,

$$F_N = F_2 - F_1 = e \frac{\mu_0 A_g N^2}{4} \left( \frac{i_2^2}{g_2^2} - \frac{i_1^2}{g_1^2} \right) \quad (5)$$

where  $i_1$  and  $i_2$  are the currents in magnets 1 and 2, and  $g_1$  and  $g_2$  are the gap distance between the mass of the rotor and magnets 1 and 2 respectively. The thickness on the either side of the bearing may be written as,

$$g_1 = g_0 - x \quad \text{and} \quad g_2 = g_0 + x \quad (6)$$

where the steady state gap thickness is  $g_0$  assuming that the rotor is centered in the axis, and  $x$  represents a perturbation in the position of the rotor measured from the center. The difference in sign is because when the rotor moves towards any of the magnets, moves away from the other one. In a similar fashion, the currents  $i_1$  and  $i_2$  can be expressed as,

$$i_1 = i_b - i_p \quad \text{and} \quad i_2 = i_b + i_p \quad (7)$$

Substituting Eq. (6) and Eq. (7) into Eq. (5), results in the following,

$$F_N = \frac{e \mu_0 A_g N^2}{4} \left[ \frac{(i_b + i_p)^2}{(g_0 + x)^2} - \frac{(i_b - i_p)^2}{(g_0 - x)^2} \right] \quad (8)$$

The linearized model of the net force  $F_N$  assumes that the perturbation current  $i_p$  and the perturbation  $x$ , are small compared to the bias current  $i_b$  and the nominal gap  $g_0$ , respectively. This allows the exclusion of the higher order terms of the perturbation current  $i_p$  and the perturbation position  $x$ , resulting in the following equation,

$$F_N = \left( \frac{e \mu_0 A_g N^2 i_b^2}{g_0^2} \right) i_p - \left( \frac{e \mu_0 A_g N^2 i_b^2}{g_0^3} \right) x \quad (9)$$

Magnetic actuator forces change with both current and air gap thickness. The change due to a change in coil current  $K_i$ , called the current stiffness gain, is the more important factor for magnetic bearings. Alternatively, the change in force due to a change in air gap thickness  $K_x$  (corresponding to a change in rotor position) is called the position stiffness. The current stiffness within the linear range, for all four air gaps in a double acting bearing, is defined as,

$$K_i = \frac{\partial F_N}{\partial i_p} = e \frac{\mu_0 A_g N^2 i_b^2}{g_0^2} \quad (10)$$

The current stiffness is positive for a magnetic bearing because an increased force in one direction is countered by an increased current on the other side which tends to oppose the external force on the moving component. The linearized expression for the current stiffness, Eq. (10), is independent of the perturbation current but linearly related to the bias current. Thus, the magnetic actuator should not be designed with a very low bias current to avoid poor response when a change in force is required. If  $i_b$  is one half of the saturation value, the dynamic range of the actuator is a maximum.

The next parameter is the position stiffness. This parameter, for all four air gaps in a double acting bearing, is defined as,

$$K_x = -\frac{\partial F_N}{\partial x} = -e \frac{\mu_0 A_g N^2 i_b^2}{g_0^3} \quad (11)$$

The position stiffness is negative. As the moving component moves close to one side, the force increases tending to pull it further in that same direction, unlike a mechanical spring tends to return it to a center.

### 3. ELETRONIC FEEDBACK CONTROL CIRCUIT

An active magnetic bearing system is required to maintain stability of the bearing-rotor system. The control system takes signals provided by the sensors, located adjacent to the actuators, and computes the necessary stabilizing current request. Amplifiers then provide the requested current to the actuators, which creates the stabilizing forces in the form of electromagnetic flux. This “feedback loop” is updated thousands of times per second. The Fig. (3) gives a block diagram of a single radial bearing control axes within a digital controller system. In addition to the stabilizing feedback loop, “open loop” control can be used to minimize unbalance-induced shaft whirl or minimize the vibration transmitted to the bearing houses. In open loop control, the active nature of the magnetic bearings is used to adaptively cancel the synchronous components of either the measured shaft position or the bearing current. It is important to note that “open loop” control alone cannot provide stable levitation; i.e., it only can be used once the system is stabilized through the feedback control action.

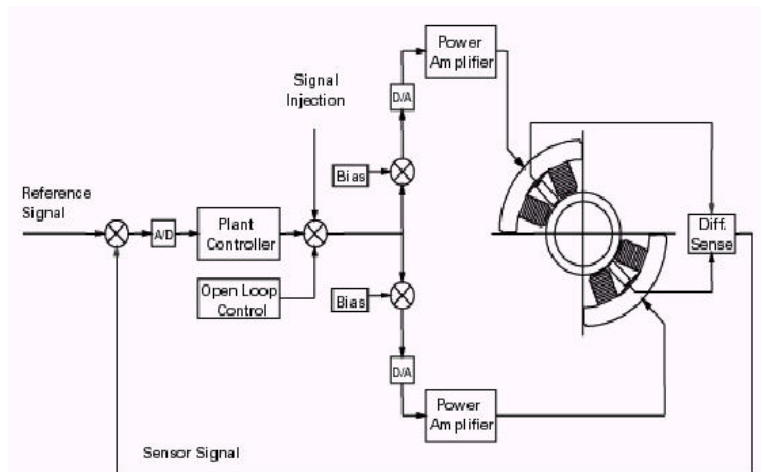


Figure 3. Single axis closed loop control block for radial bearing.  
(Diagram courtesy of Revolve Magnetic Bearing Incorporated)

As it can be seen in the Fig. (3) the electronic circuit, which controls the current in the stator coils, has three basic components: sensor, controller and power amplifier. Eventually low pass filter also can be used. It determines coil current in the actuator based upon the rotor position. The

general equation (employing Laplace transforms, where  $s$  is the complex frequency) for the control circuit is,

$$i_p(s) = G(s)x(s) \quad (12)$$

where  $G(s)$  is the overall controller transfer function which expresses the relationship between the output perturbation current, and input shaft position. If there no feedback controller employed, the negative position stiffness  $K_x$  of the actuator from Eq. (11) shows that the actuator is unstable. Therefore, the primary purpose of the feedback control is to stabilize the rotor and keep it centered. The transfer function  $G(s)$  is composed by a series of component transfer functions multiplied together, and can be written as,

$$G(s) = a_G(s) + ib_G(s) \quad (13)$$

where  $a_G$  and  $b_G$  represent the real and imaginary part of the transfer function respectively. This transfer function multiplied by the position  $x$  yields the control current  $i_p$ . Considering all components of the circuit, the complete transfer function is given by,

$$G(s) = G_S(s)G_F(s)G_{PID}(s)G_{AM}(s) \quad (14)$$

where  $G_S(s)$ ,  $G_F(s)$ ,  $G_{PID}(s)$  and  $G_{AM}(s)$  are the transfer functions of the position sensor, low pass filter, PID filter and power amplifier, respectively.

### 3.1. Position Sensor

Position sensors used to continuously monitor rotor position for magnetic bearing include eddy current sensor, induction sensor, optical sensor, capacitance sensor and others. The eddy current sensors are the most commonly employed, and the changes in the reluctance across the magnetic gap as detected by de position sensor indicate the opening or closing of the gap. The sensor has a small output voltage proportional to the shaft position, and the transfer function of the sensor system considering it behaves linearly throughout the range of motion within the stator is simply given by,

$$G_S(s) = V_x(s) / x(s) \quad (15)$$

In a radial magnetic bearing, the sensor should be placed as close as physically possible to the bearing location to avoid control problems. A particular problem arises when a shaft node point, associated with a particular rotor natural frequency, is located between the sensor and bearing.

### 3.2. Low Pass Filter

The low pass filter is used to reduce the controller's high frequency gain above the bandwidth of the hardware and at least one must be used for the bearing to operate properly. The low pass filter also allows for the bearing to operate quietly by attenuating high frequency electrical noise. A second order low pass filter of the form,

$$G_F(s) = \frac{V_F}{V_x} = \frac{\mathbf{w}_F^2}{s^2 + 2\mathbf{x}_F \mathbf{w}_F s + \mathbf{w}_F^2} \quad (16)$$

can be used to model the low pass filter where  $V_F$  is the output voltage of the filter,  $V_x$  is the input position voltage,  $w_F$  is the filter cutoff frequency,  $x_F$  is the filter damping ratio and  $s$  is the complex frequency variable. The damping ratio ( $x_F$ ) and filter cutoff frequency ( $w_F$ ) must be properly selected in the control system.

### 3.3. Proportional, Integral and Derivative (PID) Filter

The PID (proportional-integral-derivative) control is the most commonly used algorithm for magnetic bearings. The standard continuous PID transfer function form is given by,

$$G_{PID}(s) = \frac{V_{PID}}{V_F} = \frac{K_T(K_D s^2 + K_P s + K_I)}{s} \quad (17)$$

where  $K_T$  is the total gain,  $K_D$  is the derivative gain,  $K_P$  is the proportional gain,  $K_I$  is the integral gain and  $s$  is the complex frequency variable.  $V_{PID}$  is the output voltage of the filter and  $V_F$  is the input voltage from the low pass filter. In general, the proportional gain directly effects the bearing stiffness because it is multiplied by the position signal directly. Similarly, the derivative gain directly effects the damping of the axis because it is multiplied by the derivative of the position signal. The integral gain acts on steady offsets within the axis and provides a control signal to eliminate the offset. The total gain is simply a multiplier on all three gains simultaneously.

### 3.4. Power Amplifier

The output from the control circuit is typically a small voltage proportional to the desired current required for the bearing coils. The current is usually rather large, on the order of Amps, so a power amplifier is required for each bearing coil. The transfer function of the amplified can be expressed as,

$$G_{AM}(s) = \frac{I_c}{V_{PID}} = K_a \frac{w_A}{s^2 + \sqrt{2}w_A s + w_A^2} \quad (18)$$

where  $I_C$  is the control current to the individual magnets,  $V_{PID}$  is the input PID filter voltage,  $w_A$  is the filter cutoff frequency,  $K_a$  is the amplifier gain and  $s$  is the complex frequency variable.

## 4. MATHEMATICAL MODEL OF A ROTOR BEARING SYSTEM

A single axis within the bearing actuator actually consists of two identical opposing horseshoe magnets as shown in Fig. (4).

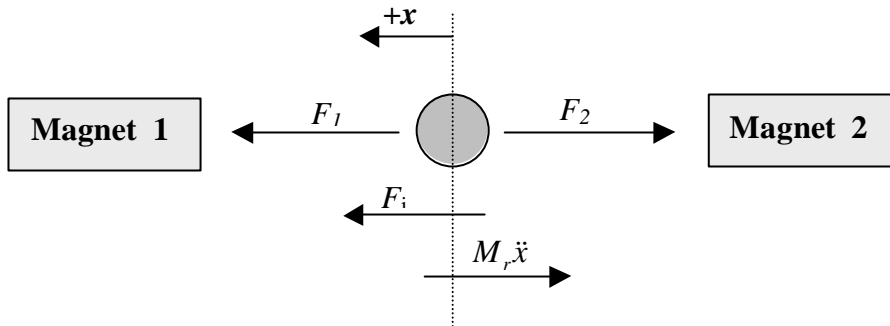


Figure 4. Single axis layout of a radial magnetic bearing

This figure shows the force from each opposing magnet,  $F_1$  and  $F_2$ , acting on the mass within a single axis. The equation of motion describing this system is given by,

$$M_r \ddot{x} + F_2 - F_1 = F_i \quad (19)$$

where  $F_i$  is an external force applied to the system and  $M_r$  is the mass of the rotor. The stiffness and damping for the axis are derived from the net force applied to the mass by the two opposing magnets. The force net ( $F_2 - F_1$ ) is given by the Eq. (9). Now, substituting the current stiffness and the position stiffness, Eq. (10) and Eq. (11), into Eq. (19) yields,

$$M_r \ddot{x} + K_x x + K_i i_p = F_i \quad (20)$$

#### 4.1. Equivalent Stiffness and Damping

The feedback controller takes advantage of a positive current stiffness to provide stability to the magnetic bearing. The controller adjusts the perturbation current  $i_p$  to the magnets to counteract the change in position detected by a sensor within the bearing. Therefore the controller transfer function simply gives a ratio of output perturbation current to input position as discussed before. The perturbation current,  $i_p$ , is also referred to as the control current,  $i$ , because it is produced by the control system and associated electronics. The controller transfer function, Eq. (13), also contains the phase information relative to the input position signal. This equation can be further simplified by substituting the complex frequency  $i\omega$  for the Laplace variable  $s$  to arrive at,

$$G(i\omega) = a_G(\omega) + ib_G(\omega) \quad (21)$$

This transfer function multiplied by the position  $x$  yields the control current  $i_p$ , which can be substituted into Eq. (20) to give,

$$-M_r X \omega^2 + [K_x + K_i(a_G + ib_G)]X = \bar{F}_i \quad (22)$$

The Eq. (22) assumes a harmonic forcing function therefore the mass acceleration has been represented as  $-X\omega^2$ . Thus, the stiffness and damping can now be determined from the net force produced by the axis position stiffness, current stiffness and controller transfer function by equating a force produced by an equivalent stiffness and damping. Equating these two forces gives,

$$(K_{eq} + C_{eq}i\omega)X = [K_x + K_i(a_G + ib_G)]X \quad (23)$$

and equating similar terms on both sides of the equation yields the equivalent axis stiffness as,

$$K_{eq} = K_x + K_i a_G \quad (24)$$

and the equivalent axis damping as,

$$C_{eq} = \frac{K_i b_G}{\omega} \quad (25)$$

The Eq. (24) and Eq. (25) represent the single axis linearized stiffness and damping values. These values change with frequency due to their dependence on the real and imaginary parts of the



controller transfer function. To successfully model the entire radial magnetic bearing system, the controller transfer function must be known.

The whole rotor bearing system can be modeled combining the rotor model with the AMB model represented by the equivalent stiffness and damping. Each part is represented in the model by its own respective formulation. The system dynamics can be written as:

$$[M_s]\{\ddot{U}\} + ([C_s] + [C_b])\{\dot{U}\} + ([K_s] + [K_b])\{U\} = \{F\} \quad (26)$$

where  $[M_s]$  is the mass matrix of the system,  $\{U\}$  is the system state vector,  $[C_s]$  is the rotor damping matrix,  $[C_b]$  is the AMB bearing damping matrix,  $[K_s]$  is the rotor stiffness matrix,  $[K_b]$  is the AMB bearing stiffness matrix and  $\{F\}$  is the system forcing vector. The matrices  $[K_b]$  and  $[C_b]$  contain the magnetic bearing properties that are calculated by the Eq. (24) and Eq. (25). The model usually contains the gyroscopic effect, which is a function of rotor rotating speed and inertia moments.

## 5. DETERMINING EQUIVALENT STIFFNESS AND DAMPING

The Fig. (5) shows the curves of equivalent stiffness and damping characteristics for each axis of a magnetic bearing from Revolve Magnetic Bearing Inc. obtained for two sets of PID control gains. All the circuit parameters used in these two cases (Case A and Case B) are indicated at right side of the figure. Using the model of the controller transfer function for each axis, Eq. (14), and the position and current stiffness of the magnetic bearing, Eqs. (10) and (11), the stiffness and damping values were determined through a computational code, which was implemented using the Matlab software. The current stiffness and the position stiffness have been calculated from the basic characteristics of the bearing to give  $K_i = 37.2$  N/Amp and  $K_x = -1.45$  E5 N/m. It can be seen that there are great differences between the stiffness and damping results of the Case A and Case B, as a function of PID filter gains taken. For rotor dynamic analysis it is reasonable taking the stiffness for the magnetic bearing as the average value over the frequency range of analysis. In the cases A and B, the average values over 0 to 100 Hz should be  $2.9$  E4 N/m and  $1.1$  E5 N/m respectively. On the other hand, the damping value can be taken asymptotically, approaching, in the cases A and B of the values  $100$  Ns/m and  $52$  Ns/m.

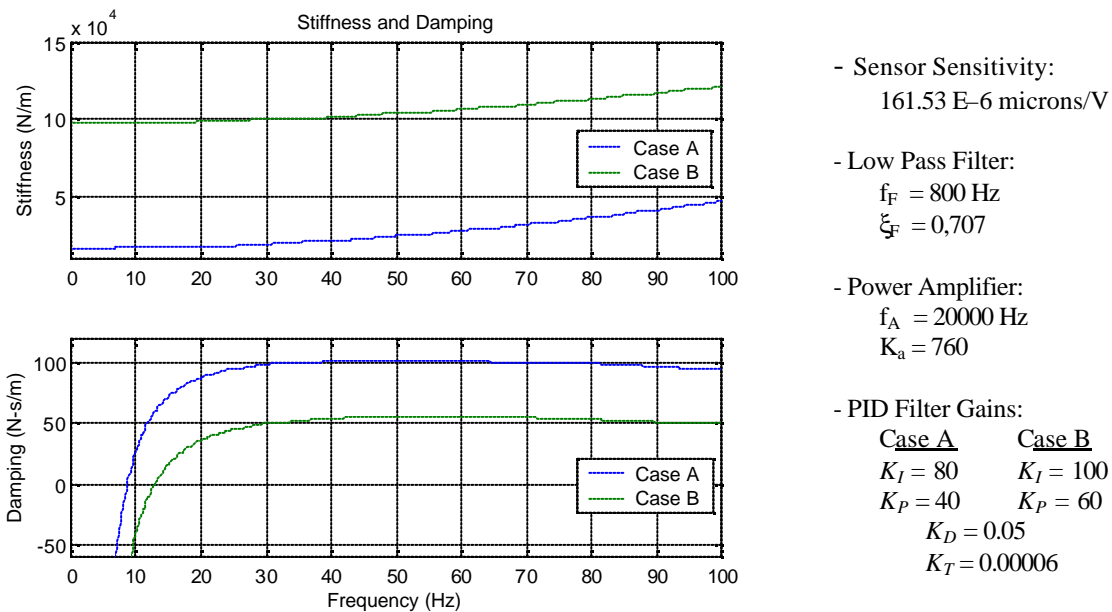


Figure 5. Equivalent stiffness and damping characteristics, and the parameters of the control circuit

## 6. CONCLUSIONS

In this article it is presented a procedure to calculate the equivalent stiffness and damping of an active magnetic bearing. It can be seen that the equivalent stiffness and damping are completely dependent of the gains given to the PID control parameters, as well as the characteristics of the sensor, low pass filter and power amplifier of the control circuit. Thus, different values for equivalent stiffness and damping can be obtained in function of the PID control parameters utilized, and this dependence permits to modify the dynamic response of the system in a rotor dynamic analysis. A computational code can be easily implemented to determine the controller transfer function, Eq. (14) and the equivalent stiffness and damping, Eq. (24) and Eq. (25). Also, it can be seen that the equivalent stiffness and damping are given as a function of the frequency. In practice, the value of the equivalent stiffness can be taken as the average over the frequency range of analysis and the value of the equivalent damping can be taken asymptotically from the curve.

## 7. ACKNOWLEDGMENTS

The author would like to acknowledge the FAPESP and FUNDUNESP, which have granted funds for development and publications of research works.

## 8. REFERENCES

- Allaire, P. E. et al, 1993, "Magnetic Bearings", STLE Handbook of Tribology and Lubrication", Vol. III.
- Beale, S. et al, 1992, "Adaptive Forced Balancing for Magnetic Bearing Systems", ", Third International Symposium on Magnetic Bearings, Alexandria, USA, pp. 601-611.
- Hawkins, L. A. et al, 1991, "The Rocketdyne Multifunction Tester: Operation oof a Radial Magnetic Bearing as an Excitation Source", ASME DE-Vol. 35, Rotating Machinery and Vehicle Dynamics, Miami, USA, pp. 201-207.
- Hope, R. W. et al, 1997, "Adaptive Vibration Control of Magnetic Bearing Equipped Industrial Turbomachinery", Proceedings of MAG' 97, Alexandria, USA, pp. 251-260.
- Kasarda, M. E. F., 2000, "An Overview of Active Magnetic Bearing Technology and Applications", The Shock and Vibration Digest, Vol. 32, N. 2, pp. 91-99.
- Knospe, C. R. et al, "Adaptive On-Line Rotor Balancing Using Digital Control", Proceedings of MAG' 93, Alexandria, USA, pp. 153-164.
- Ku, P. R. and Chen, H. M., 1993, "Optimum Shaft Balancing at a Rotor Bending Critical Speed with Active Magnetic Bearings", Proceeding of MAG' 93, Alexandria, USA, pp. 165-174.
- Nonami, K. et al, 1998, "Unbalance Vibration Control of Magnetic Bearing Systems Using Adaptive Algorithm with Disturbance Frequency Estimation", Sixth International Symposium on Magnetic Bearings, Massachusetts, USA, pp. 663-672.
- Redmond, I., 1992, "A New Approach to Flexible-Shaft Vibration Control", Third International Symposium on Magnetic Bearings, Alexandria, USA, pp. 329-338.
- Schweitzer, G. and Lange, R., 1976, "Characteristics of a Magnetic Rotor Bearing for Active Vibration Control", Paper N. C239/76, First International Conference on Vibration in Rotating Machinery, Cambridge, UK.
- Yamaishi, K., 1997, Applications and Performance of Magnetic Bearing for Water Turbine and Generator", Proceedings of MAG' 97, Alexandria, USA, pp. 25-34.